Pearl grafting: tracking the biological origin of nuclei by straightforward immunological methods.

Nelly Schmitt, Frédéric Marin, Jérôme Thomas, Laurent Plasseraud, Marina Demoy-Schneider

DOI: 10.1111/are.13499

ORIGINAL ARTICLE

WILEY Aquaculture Research

Pearl grafting: Tracking the biological origin of nuclei by straightforward immunological methods

Nelly Schmitt[1] | Frédéric Marin[2] | Jérôme Thomas[2] | Laurent Plasseraud[3] | Marina Demoy-Schneider[1]

[1]UMR 241 Ecosystèmes Insulaires Océaniens, Equipe Etude Intégrée des Métabolites Secondaires (EIMS), Université de la Polynésie française, Tahiti, French Polynesia

[2]Laboratoire CNRS UMR 6282 «Biogéosciences», Université de Bourgogne - Franche Comté (UB-FC), Dijon, France

[3]Institut de Chimie Moléculaire de l'Université de Bourgogne (ICMUB), UMR CNRS 6302, Université de Bourgogne - Franche Comté (UB-FC), Dijon Cedex, France

Correspondence
Nelly Schmitt, University of French Polynesia, Tahiti, French Polynesia.
Email: nelly.schmitt@upf.pf
and
Frédéric Marin, Laboratoire CNRS UMR 6282 «Biogéosciences», Université de Bourgogne - Franche Comté (UB-FC), Dijon, France.
Email: frederic.marin@u-bourgogne.fr

Funding information
Université de la Polynésie française; Direction des ressources marines de Polynésie française

Abstract

French Polynesia is renowned for the production of Tahitian black pearl. These gems are obtained by grafting a nucleus into the gonad of a receiving oyster together with a graft, i.e. a small section of mantle tissue of a donor oyster. This procedure initiates the formation of a pearl sack around the nucleus, and subsequently, the deposition of concentric layers of nacre. The nucleus plays a key-role in pearl formation and its characteristics influence markedly the quality of the final product. As it is manufactured from mollusc shells, it contains a small percentage of organics. In the present paper, we used a set of biochemical techniques to characterize and compare the organic matrices from two types of nuclei that are currently used in French Polynesia: that from the freshwater mussel *Amblema sp*., and that from the pearl oyster *Pinctada sp*. To this end, we extracted the matrices from nuclei and performed FT-IR, monodimensional electrophoresis, and enzyme-linked immuno-sorbent assay (ELISA). Our data show that the matrix associated with *Amblema* nuclei has a very different biochemical signature from that of *Pinctada* nuclei, a fact that may explain the improved tolerance of grafted oysters to nuclei of *Pinctada* origin. In the absence of complex physical methods of investigation, simple immunological techniques and FT-IR performed on the extracted organic matrix are extremely reliable and effective for discriminating nuclei from these two sources. We assert that such techniques can be used as a diagnostic test to track unambiguously the biological origin of nuclei to avoid fraud.

KEYWORDS
Amblema plicata, ELISA, matrix proteins, nucleus, pearl oyster, *Pinctada margaritifera*

1 | INTRODUCTION

With a production fluctuating between 8 and 10 tons per year, French Polynesia is renowned all over the world for its Tahitian black pearl, representing about US$120 million per year, the second source of income of the archipelago after tourism (Southgate, 2007; Tisdell & Poirine, 2008). These priceless gems are produced according to the grafting procedure invented by Mise-Nishikawa on the Akoya pearl oyster (*Pinctada fucata*) and improved by Mikimoto and his company at the beginning of the twentieth century, before being extended to other pearl oyster species (Herbaut, Hui, Herbaut, Remoissenet & Boucaud, 2000; Nagai, 2013; Taylor & Strack, 2008): in French Polynesia, cultured pearls are obtained by incising the gonad of a receiving oyster - the black-lipped pearl oyster *Pinctada margaritifera* - and by placing in it a mineral bead, the nucleus, together with a graft, i.e. a few square millimetres of the mantle epithelium removed from a selected donor oyster of the same species (Ellis & Haws, 1999). From a cellular viewpoint, this procedure initiates the development of a thin mineralizing epithelium around the nucleus, in 30–50 days (Awaji & Suzuki, 1995; Herbaut et al.,

2000). Once formed, this pearl sack deposits first a film of organic materials, then concentric layers of nacre tablets around the nucleus at a rhythm of few micrometres per day (Caseiro, 1995). A marketable pearl, corresponding to a deposited nacre thickness above 0.8 mm, is usually produced after 18 months. Because pearl formation takes time, this process can be interrupted at any moment by deleterious events of a very different nature: expulsion of the nucleus, bad post-graft recovery of oyster leading to mortality, changing food availability, hurricanes, pollution, colonization of the shell by marine boring organisms, predation or viral/bacterial infection (Hine & Thorne, 2000; Humphrey, 2008; Mao Che et al., 1996). This explains why the production of a "top gem" pearl – a pearl that is ranked the highest according to five quality criteria – is a rare event that justifies a high price of the final product.

Among the pivotal parameters that markedly impact the commercial value of the final product, one finds the characteristics of the nucleus (Roberts & Rose, 1989). Manufactured from mollusc shells, the nucleus plays a key-role, in particular during the early steps of pearl formation, where its nature, size and surface properties can influence, among other variables, the rate of rejection, the quality of the pearls, their shape and the number of surface defects (Cochennec-Laureau et al., 2010): indeed, similarly to every shell, the nucleus contains a small percentage of organics that can induce or not immune response of the grafted oyster. The production of nuclei goes as follows: after abrasion of the outer layer, shells are first cut into strips, which are subsequently cut into cubes. The cubes are manually shaped in spheres, which are further processed into a grinder to achieve a perfect sphericity (Taylor & Strack, 2008); the nuclei are then sorted according to their size and to their grade, before being cleaned, dried and conditioned in bags for commercialization. In some cases, extra-steps include nucleus coating with antibiotics or antibacterial peptides to decrease post-grafting mortality (Cochennec-Laureau et al., 2004; Norton, Lucas, Turner, Mayer & Newnham, 2000).

In most of the cases, nuclei used for the grafting process are manufactured from shells of American freshwater mussels (such as pigtoe, washboard, butterfly, three ridge and dove shells) of the unionid family, representing ten different species found in Mississippi and Tennessee watersheds (Cartier & Krzemnicki, 2013; Superchi, Castaman, Donini, Gambini & Marzola, 2008). These shells are thick, solid and exhibit good drillability properties, while their specific gravity, thermal properties and light colour make them appropriate for grafting. However, inventories of American freshwater mussel shells are down and, in the long term, this resource is not secured (Strayer, 2008; Taylor & Strack, 2008). Recently, in French Polynesia, the use of nuclei manufactured from shells of *Pinctada* sp. has been successfully developed as a credible alternative to the endangered Mississippi nuclei. In particular, a pilot study carried out at the Ifremer (COP, Vairao, French Polynesia) between 2007 and 2009 showed that a significant difference exists in pearl quality and shape when nuclei manufactured from *Pinctada sp* shell are used rather than those from *Amblema sp* (2009 activity report of LEAD-PF dpt., *unpublished*).

The aim of the present paper is to compare the organic matrices extracted from two types of nuclei: that of *Amblema plicata*, the current American freshwater unionid mussel, and that of *Pinctada* sp., the pearl oyster. To this end, we extracted their nucleus matrices and performed Fourier transform infrared spectroscopy (FT-IR), monodimensional electrophoresis (SDS-PAGE), and comparative immunological tests on microplates by enzyme-linked immuno-sorbent assay (ELISA). Our data show that the matrix associated with *Amblema* nuclei differ drastically from that of *Pinctada* nuclei. In the absence of heavy physical techniques of materials characterization, both immunological and FT-IR approaches give a reliable and fast response for distinguishing unambiguously the two types of nuclei; they can be consequently developed for diagnostic tests to track the biological origin of nuclei.

2 | MATERIALS AND METHODS

2.1 | Materials

The nuclei used in this study come from two genera: *Amblema* and *Pinctada*. *Amblema plicata*, the "three ridge" shell, is a bivalve of the Palaeoheterodonta sub-class. It belongs to the Unionida order and to the Unionidae family. It exhibits a nacro-prismatic shell texture that is entirely aragonitic (Petit, Davis & Jones, 1980), like all members of this clade. *Pinctada sp.*, a pearl oyster, is a bivalve of the Pteriomorphia subclass, and belongs to the Pterioida order and of the Pteriidae family. Its shell texture is also nacro-prismatic, but contrarily to *Amblema*, the outer shell layer is constituted of calcitic prisms (Erben, 1972). In both cases, nuclei are made from the more solid internal aragonitic nacreous layer.

We used four different batches of nuclei, comprising each, tens to hundreds of nuclei; two of them were from *Amblema*, the two others, from *Pinctada sp*. These batches were provided by two sources, the company "Inami" (I) and the "Service de la Perliculture" (SP): they were consequently named *Amblema* I, *Amblema* SP, *Pinctada* I and *Pinctada* SP. Their respective weight was as follows:18, 173, 140 and 22 g. Nuclei were sorted by bare eye and the few containing the transition zone to the prismatic layer (such as nuclei 5 of Figure 1) were discarded from further analyses. Only nuclei that exhibited homogeneous colours, corresponding solely to the nacreous layer, were selected.

2.2 | Nuclei observation and preparation

Nuclei of the four batches were cleaned with bleach (sodium hypochlorite, 0.26% active chlorine) during 48 hr, at room temperature, under gentle shaking. They were thoroughly rinsed with Milli-Q water and dried at 37°C. Prior to cleaning, few of them were selected for macro-pictures. In addition, few more were fragmented by mechanical shocks, and the fresh surfaces were cleaned in ultrasound bath before being dried and carbon sputtered. They were subsequently observed with a Scanning Electron Microscope (JEOL 6400; JEOL Europe SAS, Croissy/Seine, France) in secondary electron mode.

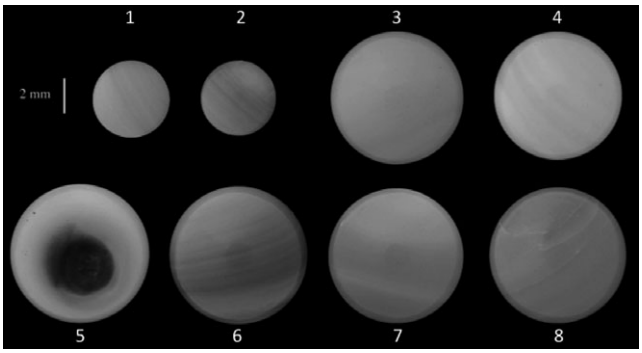

FIGURE 1 Few examples of the nuclei from the different batches used in this study. Samples of the top line (1–4) are nuclei from *Amblema plicata*, that of the bottom-line (5–8), from *Pinctada*. Nuclei 1, 2, 5, 6 correspond to SP batch (Service de la Perliculture). Nuclei 3, 4, 7, 8 to I batch (Inami). Note that nucleus 5 contains a little bit of the transition zone to prismatic calcitic layer (brown spot in the middle). Such nuclei were discarded from our analyses. The nuclei of *Amblema* SP (1, 2), of *Pinctada* SP (5, 6) and of *Pinctada* I (7, 8) batches exhibit colours varying from whitish to brownish. Nuclei from *Amblema* I (3, 4) batch are all white. The colour of the nuclei cannot be taken into account for discriminating the nuclei of *Amblema* and of *Pinctada* sources

Nuclei of the four batches were coarsely ground manually with a pestle and a mortar, before being powdered with an electric mortar grinder (Pulverisette 2; FRITSCH, Idar-Oberstein, Germany). The resulting powders were sieved to select particles with a grain size below 200 μm. We checked by FT-IR that the powders of all batches exhibited the typical aragonite spectrum, with peaks at 700, 713, 858 and 1,477 cm^{-1}.

2.3 | Extraction of nucleus matrices by decalcification

For extracting the nucleus matrices of the four batches, we employed two decalcification procedures: one with cold dilute acetic acid, one with concentrated EDTA, depending on the subsequent analytical procedures applied on the extracted matrix (Marin, 2003; Marin, Gillibert, Wesbroek, Muyzer & Dauphin, 1999): in the first case, the matrix was analysed by sodium dodecyl sulphate polyacrylamide gel electrophoresis (SDS-PAGE) and Fourier transform infrared spectroscopy (FT-IR). In the second case, the matrix was analysed on microplates by the ELISA.

For the acetic acid extraction, the powder of each batch (from 12 to 15 g) was suspended in Milli-Q water, under constant stirring, at 4°C, then, slowly decalcified overnight with cold dilute acetic acid (10%vol.vol^{-1}), which was progressively added (100 μl every 5-s) with an electronic burette (Titronic Universal; SCHOTT, Mainz, Germany). At the end of the decalcification, the resulting solution was centrifuged for 15 min at 3,900 *g*. The supernatant containing the acid-soluble matrix (ASM) was separated from the pellet, i.e. containing the acid-insoluble matrix (AIM). The AIM was scrupulously rinsed by a series of resuspension in Milli-Q water/centrifugation (five cycles), then lyophilized and weighed (direct weighing of the lyophilisates). The ASM was filtered on an NALGENE filtration device (5 μm cutoff) then its volume was reduced by ultrafiltration, using a 400 ml AMICON cell with a 10 kDa cutoff membrane. Then, the concentrated solution (about 10 ml) was dialysed for 2 days at 4°C in a Spectra/Por tube (cutoff 1,000 Da) against Milli-Q water, with five water changes. The solution was finally lyophilized overnight.

In the second case, we employed a simplified extraction procedure that allows direct testing of the extracts with ELISA microplates: each of the four nucleus matrices was extracted by placing 300 mg powder in a tube and adding 3 ml of 20% EDTA (wt.vol^{-1}), pH 8. The four tubes were gently shaken on a rotating device (APELEX), allowing the powder to dissolve overnight at room temperature. The tubes were briefly centrifuged, to separate the EDTA-insoluble matrix from the supernatant, which was directly tested in ELISA microplate, without requiring the removal of EDTA salts.

2.4 | Nucleus matrices characterization by Fourier-transform infrared spectroscopy

FT-IR spectra of the four AIM and of the four ASM were recorded from minute chips of lyophilized nucleus matrices, with a BRUCKER Vector 22 instrument equipped with a SPECAC Golden Gate Attenuated Total Reflectance (ATR) device (SPECAC, Orpington, UK) in the 4,000–500 cm^{-1} wavenumber range. Per sample, 10 scans were performed, at a spectral resolution of 4 cm^{-1}. The assignment of the different absorption bands was obtained by comparison with previous spectra descriptions available in the bibliography (Kanold et al., 2015).

2.5 | Nucleus matrices characterization by monodimensional gel electrophoresis

Conventional SDS-PAGE was performed to analyse the matrix components, under denaturing conditions, on 12% polyacrylamide mini gels (Mini-Protean 3; BIO-RAD, Hercules, CA, USA), according to the manufacturer's instructions. Lyophilisates of the ASM were directly dissolved in 2× Laemmli sample buffer (LSB) containing β-mercaptoethanol and in the equivalent volume of Milli-Q water, to reach a final concentration of 2 μg/ml, before being heat denatured for 5 min at 100°C. For the AIM, 10 mg of lyophilisates were resuspended in 100 μl Milli-Q water and 100 μl LSB and heat denatured 5 min at 100°C. As AIM only partly dissolves in these conditions, the supernatant is referred to as the Laemmli-soluble acetic acid-insoluble matrix (LS-AIM); it represents only a part of the total AIM. Samples were loaded on gels, which were subsequently run 15 min at 100 V then about 1 hr at 150 V. For visualization of proteins, gels were stained with silver nitrate according to the protocol of Morrissey (1981). Fresh gels were scanned and then dried with a BIO-RAD gel dryer.

2.6 | Nucleus matrices characterization by ELISA

The four soluble EDTA-extracts of the nuclei were tested by conventional ELISA (Enzyme-Linked Immuno-Sorbent Assay; Clark & Adams, 1977) for checking their capacity to cross-react with a set of

polyclonal antibodies elicited in rabbit against unfractionated acetic acid-soluble mollusc shell matrices. The target antigens of these antibody preparations were: the ASM of the prismatic layer of *P. margaritifera* (K5087) and the ASM of the nacreous layer of *P. margaritifera* (K5088). These antibodies were used in former studies (Marin, Muyzer & Dauphin, 1994; Marin et al., 1999; Pavat et al., 2012). In addition, we used a much more specific antibody elicited against a purified shell matrix protein of the bivalve *Pinna nobilis*, caspartin, and developed for a former project (Marin et al., 2005). Negative controls were performed with pre-immune sera in the same experimental conditions as for antibodies.

In brief, the EDTA-extracts (100 μl), obtained as described in the paragraph "Extraction of nucleus matrices by decalcification", were directly incubated in an NUNC Maxisorp 96 well microplate (90 min, 37°C). After the blocking step (0.5% wt.vol^{-1} gelatin in TBS, 30 min, 37°C), the microplate was incubated (90 min, 37°C) with the antibody solutions that were serially diluted (1/1,000, 1/3,000, 1/9,000, 1/27,000 for anti-caspartin and 1/500, 1/1,500, 1/4,500, 1/13,500 for all other antibodies). It was subsequently incubated (90 min, 37°C) with the secondary antibody (goat anti-rabbit, SIGMA A3687, diluted 30,000 times). Rinsing steps with TBS containing 0.05% (vol.vol^{-1}) Tween 20 (using a manual NUNC Immuno Wash 12 microplate washer) were performed after incubation of the antigens, of the 1st antibody and of 2nd AP-conjugate antibody. The microplate was revealed with the substrate solution, consisting of 4-nitrophenyl phosphate (Sigma N9389, 5 mg tablet per 10 ml solution) dissolved in a water:diethanolamine solution (10:1), pH 9.8 that was kept 30 min at 37°C before use. The microplate was incubated 15 min at 37°C and read with a multichannel spectrophotometer (BIO-RAD, model 680) at 405 nm at regular intervals and the best reading was selected. Colour development was stopped by the addition of 100 μl sodium hydroxyde (1 M) in each well. The whole test was repeated at least three times. Data were expressed in percentage of cross-reactivity, the highest signal for each antibody (usually $1 < OD < 1.5$) being equal to 100%, while the background reactivity (OD about 0.04–0.05) was considered as 0%.

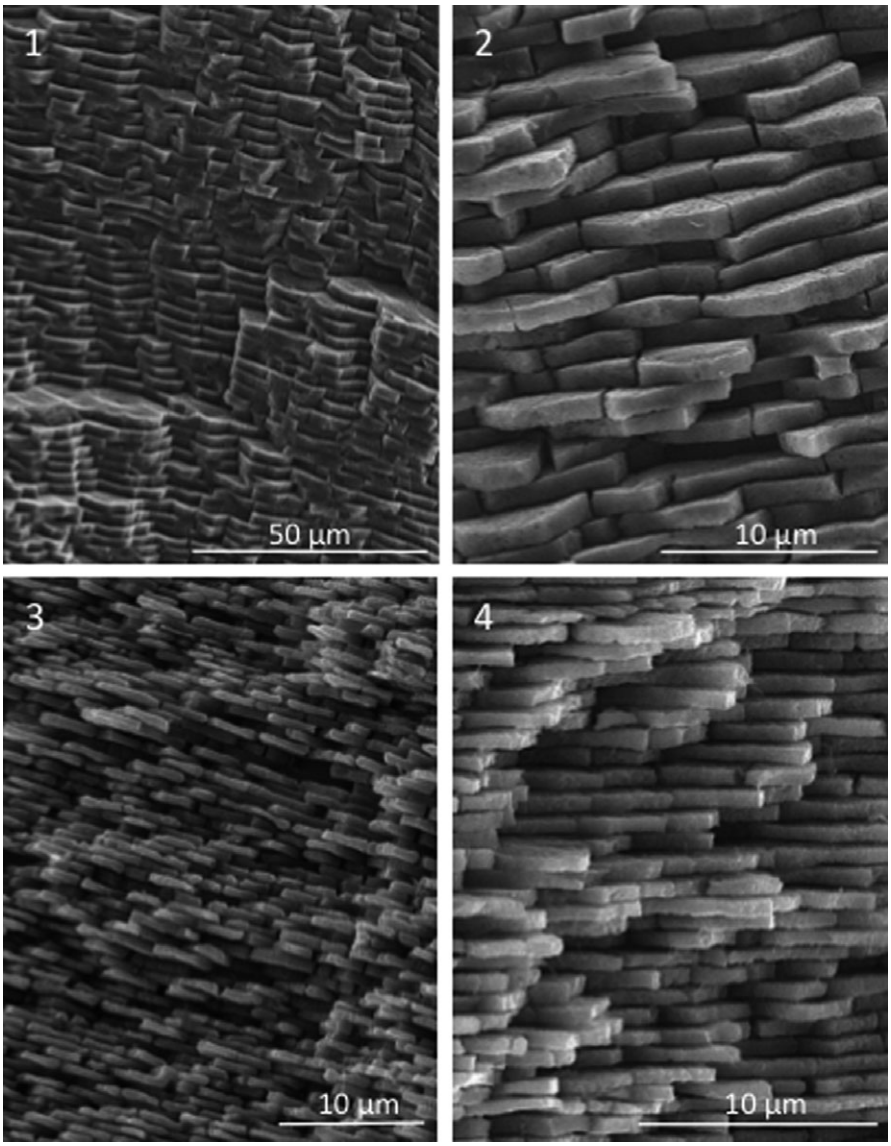

FIGURE 2 SEM micrographs of fresh fractures of the nucleus nacre of *Amblema* (1, 2) and of *Pinctada* (3, 4). 1, 3: batch Service de la Perliculture (SP); 2, 4: batch Inami. In all cases, nacre is characterized by flat tablets of aragonite, arranged in a brick-wall manner

3 | RESULTS

3.1 | Macroscopic and microscopic observations of nuclei

Macro-photos of the studied nuclei are shown in Figure 1: they represent few examples of nuclei taken from the four batches. A bare eye observation does not allow differentiating the *Amblema* nuclei from the *Pinctada* ones, especially when the nuclei are not pigmented (white, see samples 3, 4 and 7).

SEM pictures of Figure 2 show that the two types of nuclei (*Amblema*, *Pinctada*) are very similar and do not exhibit marked differences: both exhibit the "brick-and-mortar" structure, typical of bivalve "sheet" nacres found in pteriomorphid and paleoheterodont subclasses. A closer observation shows that nacre tablets of *Amblema*, of about 1 μm, are slightly thicker and less flexuous than that of *Pinctada*. These latter exhibit a mean thickness about 0.5 μm and are "flatter" (lower thickness/width ratio). At low magnifications (<10,000 times), these differences are, however, tenuous and cannot be easily utilized as discriminant parameters in a blind recognition test.

3.2 | Matrix extraction and bulk characterization by FT-IR

Table 1 summarizes the amount of acetic acid insoluble matrices (AIM) extracted from the four batches. We did not quantify the amount of ASM. Our data show that the quantity of AIM extracted from *Amblema* nuclei (varying from 0.22 to 0.4 wt-%) is significantly lesser than that extracted from *Pinctada*, which represents between 0.7 and 0.9%.

Figure 3 shows the FT-IR spectra obtained from lyophilisates of AIM (Figure 3a) and of ASM (Figure 3b) of the Inami and of the SP batches. The curves are expressed in % transmittance. For all samples, we observe the classical series of peaks that are typical of protein backbone: amide A (N-H stretching) at 3,269–3,273 cm^{-1}; Amide I (C = O stretching) at 1,624–1,646 cm^{-1}; Amide II (C-N stretching/N-H bending) at 1,515–1,534 cm^{-1}; amide III (C-N stretching/N-H bending) at 1,220–1,230 cm^{-1}. Note that the amide III peaks of the four ASMs are slightly broadened, suggesting fusion of two signals.

Apart from the protein peaks, we observe series of supernumerary peaks between 2,800 and 3,000 cm^{-1} (accentuated in ASMs, attenuated in AIMs), between amide II and amide III peaks, and between 1,220 (amide III) and 850 cm^{-1}. Peaks at 2,922–2,932 cm^{-1}, at 1,446–1,447 cm^{-1}, and at 1,034–1,040 cm^{-1} may be attributed to the νC-H (alkanes, −CH3 groups), νC-H (asymmetric and symmetric) and νC-O (polysaccharides) vibrations respectively. One has to note that the polysaccharide peaks, at 1,034–1,040 cm^{-1}, exhibits high amplitude for all ASMs while they appear to be minor for all AIMs. Reversely, a peak at 1,151–1,163 cm^{-1} is extremely accentuated for AIMs, while it is hardly marked in all ASMs. This peak may indicate the presence of sulphate or phosphate groups, in connection to the occurrence of small peaks at 618–624 and around 550 cm^{-1} (De Paula & Silveira, 2009; Rhee & Tanaka, 2001).

Interestingly, our FT-IR data allow comparisons between I batch (Inami) and SP batch (Service de la Perliculture): remarkably, the two *Pinctada* AIM give almost superimposable spectra (Figure 3a), and the two *Pinctada* ASM, too (Figure 3b). For the *Amblema* nuclei, the spectra, although very close, are not completely superimposable and slight differences are observed between the I and SP batches: for AIMs, in the 1,222–1,163 cm^{-1} (difference of amplitudes of the two peaks) and in the 500–650 cm^{-1} regions; for ASMs, in the 2,932 cm^{-1} region (νC-H vibration of alkanes) where the amplitude of the peak is increased for the SP ASM, and in the 1,300–1,400 cm^{-1} region, where a supernumerary small peak is observed at 1,320 cm^{-1} for the same ASM. These differences may be due to different proportions of pigments in I and SP batches of *Amblema* nuclei: indeed, we noted a difference of colour between *Amblema* SP nuclei, which are slightly coloured (whitish to brownish, see Figure 1, nuclei 1 and 2) and the *Amblema* I ones, which are all invariably white, i.e. not pigmented (Figure 1, nuclei 3 and 4). To corroborate this explanation, it was shown that pigments of the shell of marine snails were characterized, among other identification criteria, by a peak at 2,980 cm^{-1} corresponding to the νC-H vibration of alkanes (Williams et al., 2016), similarly to the peak observed in the ASM of the *Amblema* SP batch.

A comparison between the ASM spectra of *Pinctada* and *Amblema* nucleus matrices shows seven noteworthy differences: the amide A peak at 3,271–3,277 cm^{-1} for the *Pinctada* ASMs of both batches (I and SP) exhibits much higher amplitude than that of *Amblema* nucleus matrices. Similarly, the sharp peak at 1,400–1,405 cm^{-1} is well marked for *Pinctada* (batch I or SP) but hardly detected in the *Amblema* ASMs. In addition, four other peaks, at 1,107, 994, 922 and 851–852 cm^{-1} discriminate the *Pinctada* nucleus ASM from the *Amblema* nucleus matrices, for which these peaks are hardly marked, or absent. Finally, the zones (between 500 and 650 cm^{-1}) close to the far IR of the ASM spectra present also

TABLE 1 Quantification of the acetic acid insoluble matrices extracted from *Amblema* and from *Pinctada* nuclei, and from two types of batches: Inami and SP (Service de la Perliculture). The results (in bold) are expressed in % acid-insoluble matrix (AIM) of the total weight of nuclei

Genera→	Amblema		Pinctada	
Batches→	SP	Inami	SP	Inami
Weight of nucleus powder (grams)	15.5	12.3	15.7	14.0
Weight of AIM (milligrams)	69.8 (±1)	27.1 (±1)	142.6 (±1)	99.6 (±1)
% AIM (wt-%)	**0.45** (±0.01)	**0.22** (±0.01)	**0.91** (±0.01)	**0.71** (±0.01)

SP, Service de la Perliculture.

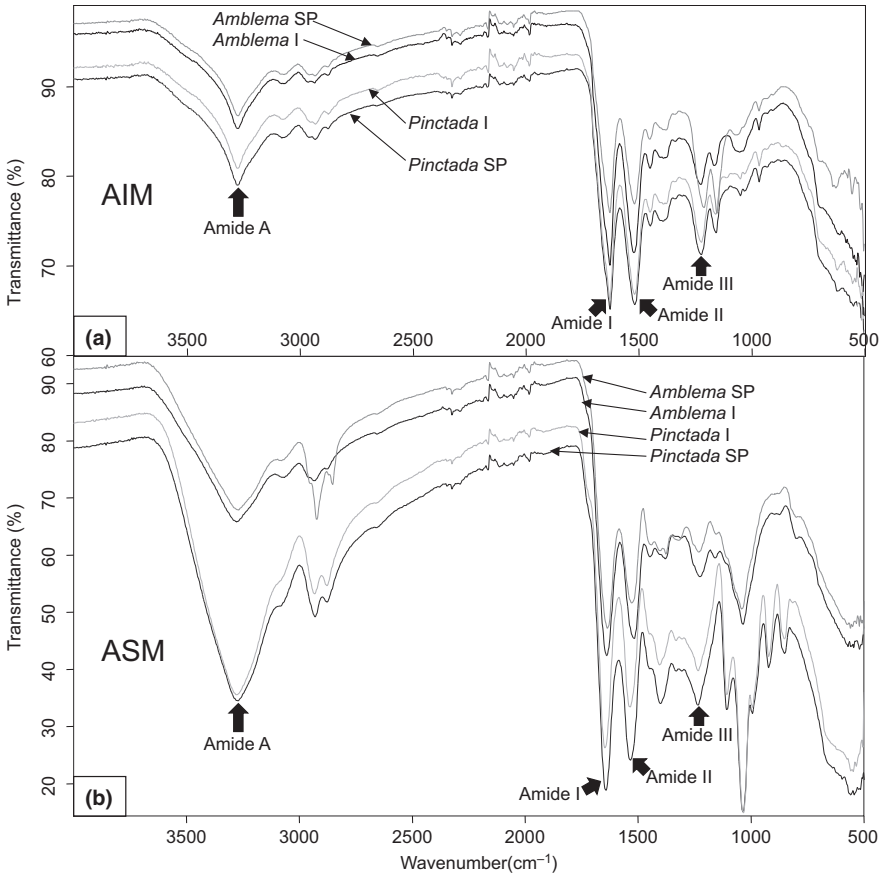

FIGURE 3 FT-IR spectra of the nucleus acid-insoluble matrix (AIMs) (a) and of the nucleus acid-soluble matrix (ASMs) (b) of *Amblema* (I and Service de la Perliculture [SP] batches) and of *Pinctada* (I and SP batches)

differences between *Pinctada* and *Amblema*. Between the *Pinctada* AIMs and that of *Amblema*, the differences are less marked: the most significant one concerns the 1,048–1,070 cm^{-1} peak, generally attributed to polysaccharides (νC-O vibrations), which is sharp and of low amplitude for *Pinctada*, while it is higher and broadened (dome-like) for *Amblema*. These observations, taken together, suggest that the matrices - in particular the ASMs - extracted from the two types of nucleus (*Pinctada*, *Amblema*) can be discriminated on the basis of FT-IR spectroscopy.

3.3 | Nuclei matrices characterization by SDS-PAGE

The ASMs and LS-AIMs were run on standard SDS-PAGE mini gels, and the results are shown on Figure 4a and b respectively. For ASMs, we observe that all samples are characterized by smeary patterns, particularly in a migration zone comprised between 70 kDa and the migration front. The two *Pinctada* ASMs which look very similar, are characterized by few discrete bands between 60 and 50 kDa, below 30 kDa, at 25, 17 and 12 kDa, while less bands, although more

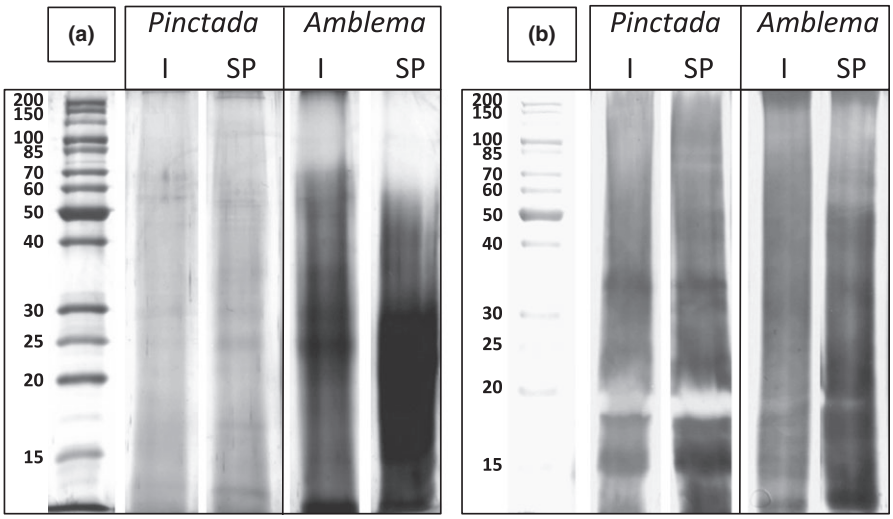

FIGURE 4 Monodimensional gel electrophoresis of the matrices extracted from *Pinctada* and from *Amblema* nuclei. The gels were stained with silver nitrate. a: Acid-soluble matrix samples; b: LS-AIM samples (Laemmli-soluble, acetic acid insoluble fraction). I: Inami batches; SP: batches from "Service de la Perliculture". The lane on the left side of each of the two gels corresponds to the molecular weight markers (unstained protein ladder, Euromedex)

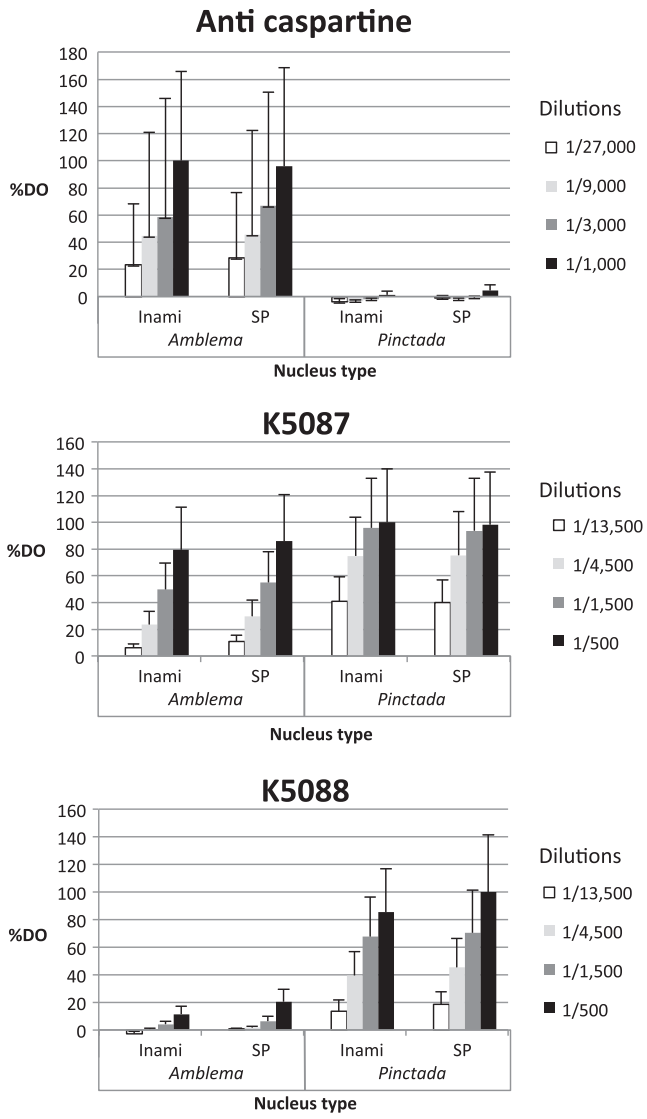

FIGURE 5 Results of the enzyme-linked immuno-sorbent assay (ELISA) experiments performed on the EDTA-soluble extracts of the *Amblema* and of the *Pinctada* nucleus matrices tested against anti-caspartin (top), K5087 antibody (middle) and K5088 antibody (bottom). Results are expressed in % reactivity ± *SD* for triplicate experiments, the highest reactivity representing 100% for each test. These three antibodies discriminate the two biological origins (*Amblema* or *Pinctada*) of nuclei. For each tested antibody, I and Service de la Perliculture (SP) batches that belong to the same biological origin react similarly

prominent but blurred, are observed for the ASM of *Amblema* (Inami batch) around 35 kDa, below 30 and at 25 kDa. The pattern of the SP batch for *Amblema* is less distinct. For LS-AIMs, the matrices of the two genera are mainly composed of non-discrete molecules that give intense smearing pattern, from the top of the gel to its migration front. However, discrete molecular weight components are also present that allow distinguishing between the matrices of the two genera: the AIMs of *Pinctada* exhibit two prominent bands at 35 and 15 kDa, and one negatively stained band below 20 kDa, while the AIMs of *Amblema* are more uniformly stained and do not exhibit negative staining; one low-molecular weight band between 15 and 10 kDa can be detected for these samples.

3.4 | Characterization of nuclei ASM by ELISA

The three histograms of Figure 5 present the results of the ELISA test obtained with three polyclonal antibody preparations tested against the nucleus ASMs of *Pinctada* and of *Amblema*: K5087, raised against the ASM of the prismatic layer of *P. margaritifera*, K5088, against the ASM of the nacreous layer of the same species, and finally anti-caspartin. These three antibodies discriminate at different degrees the ASM of the two genera: while anti-caspartin gives a strong reactivity with the nucleus ASM of *Amblema* but no reactivity with the nucleus ASM of *Pinctada*, K5088 antibody gives the reverse pattern: a strong reactivity with the nucleus ASM of *Pinctada* and no cross-reactivity with the nucleus ASM of *Amblema*. The K5087 antibody gives a reactivity that resembles that of K5088, although less discriminating: at low dilution (1/500), the two ASMs give high reactivity, with a higher signal for *Pinctada* ASM. At intermediate dilution (1/1,500), the reactivity of *Pinctada* ASM is maintained high while that of *Amblema* is moderate. At high dilutions (1/4,500, 1/13,500), the differences in reactivity between *Amblema* and *Pinctada* ASMs are the most significant: that of *Amblema* collapse while that of *Pinctada* stay high. Results obtained with the other polyclonal antibodies tested in this study are not shown, because they did not discriminate sufficiently the nucleus ASMs of the two sources. To conclude, two of our antibody preparations discriminate in a contrasted manner the ASMs extracted from *Amblema* and from *Pinctada* nuclei, whatever the dilution used, while our third antibody is discriminant enough when used at high dilution.

4 | DISCUSSION

In the present paper, we have investigated the overall biochemical signatures of the acetic acid soluble and acetic acid-insoluble matrices extracted from two types of nucleus beads used for grafting the Polynesian black-lip pearl oyster, *P. margaritifera*. The first type corresponds to nuclei classically manufactured from *A. plicata* shells, while the second type, to nuclei made from *Pinctada* shells. Several proteomic studies identified proteins constituents of the shell of the pearl oyster (Liu et al., 2015; Marie et al., 2012). Such an approach has not been tried yet on *Amblema*; consequently, no shell protein is known in this genus.

Our study had one main scope: to find rapid methods for discriminating the two types of nuclei. To this end, we extracted the nucleus matrices of *Amblema* and of *Pinctada*, and performed different biochemical characterization, comprising SDS-PAGE, FT-IR and finally ELISA, in order to compare their overall biochemical properties. Our data show that the nucleus matrices of *Amblema* and of *Pinctada* differ in several biochemical features.

First of all, the quantities of acetic acid-insoluble matrix (AIM) in the two types of nucleus are different, that of *Pinctada* nuclei being

close to 1 wt-%, while that of *Amblema* is about twice as less. Interestingly, these values match with published works on the nacre matrix of *P. margaritifera* on the one the hand (Marin et al., 2013), and on the nacre matrix of *Unio pictorum*, a freshwater unionoid mussel closely related to *Amblema*, on the other hand: we showed indeed that *U. pictorum* AIM represents 0.5% of the nacre weight (Marie et al., 2007). Secondly, the SDS-PAGE profiles of the *Amblema* and *Pinctada* matrices are dissimilar, although these differences are not noteworthy, due in particular to the abundance of non-discrete molecular weight macromolecules characterizing the smearing patterns of both ASMs and LS-AIMs, which blur the picture. The differences rest on few discrete molecular weight bands in the [15; 35 kDa] molecular weight range, present or absent in each of the preparations.

More reliably, important differences are recorded when FT-IR and ELISA techniques are employed on ASM extracts. At first, the FT-IR spectra of *Amblema* and of *Pinctada* ASMs differ markedly. In particular, in the (500 cm^{-1}; 1,500 cm^{-1}) spectral domain, the *Pinctada* ASM spectrum is characterized by four peaks of high amplitude, not observed in the *Amblema* samples. Secondly, the ELISA technique—when two of our antibodies, K5088 and anti-caspartin, are employed—elicits very clear "binary" signals (reactivity, no reactivity) that are opposite between the two sources of extracts. We do not know the identity of the cross-reacting epitopes in the *Pinctada* and *Amblema* ASMs, neither in terms of nature (proteinaceous, polysaccharidic?) nor in terms of structure (sequence?). However, our two polyclonal antibodies give non-ambiguous responses that are highly reproducible.

Taken together, all our data demonstrate unambiguously that the *Amblema* and *Pinctada* nucleus matrices are biochemically very different. This difference may have an impact on the higher or lesser tolerance of the grafted oyster to the foreign body, the nucleus. Although the molecular interactions between the nucleus and cells of the forming pearl sack have never been investigated in detail so far, we may suggest the following scenario: after implantation in the gonad, the surface of nucleus stays in contact with its immediate cellular environment comprising the graft, the gonad cells, conjunctive tissue cells and probably free-moving hemocytes. Because the formation of the pearl sack and the subsequent deposition of the first organic layer around the nucleus take days, this prolonged contact may be long enough to allow the release—at low dose—of diffusive factors from the nucleus. One knows that nuclei-made from shells—comprise a complex mixture of proteins (Marin, Le Roy & Marie, 2012) among which some, such as growth factors, may play key functions in cell signalling (Weiss, Göhring, Fritz & Mann, 2001; Westbroek & Marin, 1998). Thus, some of these factors, if released from the nucleus, may trigger the process of biomineralization and activate cells of the forming sack. Furthermore, the use of nuclei of the same biological origin as the implanted oyster—in the present case *Pinctada*—may allow a better tolerance, i.e. "immuno-compatibility", between gonad cells, hemocytes, graft cells and the foreign body. If this hypothesis on the "nucleus effect" was valid, it would corroborate the results of a field study conducted at the IFREMER station of Vairao, Tahiti, described in an unpublished activity report (2009 report of LEAD-PF Dpt.): indeed, this study showed that a higher proportion of "quality A" pearls was obtained when nuclei made from *Pinctada* sp shell nacre were used instead of the conventional nuclei made from *Amblema* nacre.

In conclusion, we have employed a set of simple techniques to discriminate and track the two sources of nuclei used for grafting pearl oysters in Polynesia. Contrarily to SEM observations, these techniques are relatively easy to implement and can be used in "blind assay" (i.e. when the biological source of the nuclei is not known). In particular, ELISA, following a simplified overnight extraction with EDTA as we did, gives a "visual" answer, which is remarkably reliable, in few hours, without even needing a spectrophotometric lecture. We suggest that simple identification kits—similar to pregnancy test—might be developed to this end, to detect potential frauds or misuse of inappropriate nuclei. Future proteomic studies are, however, required to obtain the nucleus protein repertoire of *Amblema* source, in order to compare it thoroughly to that of *Pinctada*. In addition, this approach will allow the identification of putative diffusible factors that may modulate the cellular response at the vicinity of the nucleus, in the few days following the graft.

ACKNOWLEDGMENTS

This study is part of a collaborative project (Groupement De Recherche ADEQUA) supported by the "Direction des Ressources Marines" of French Polynesia. It is also supported by the University of French Polynesia and by IFREMER. This work results from a short training period of N. Schmitt in the biomineralization laboratory of F. Marin in Biogéosciences, Université de Bourgogne Franche-Comté, Dijon.

AUTHOR CONTRIBUTIONS

F.M. designed the experiments and N.C. performed the biochemical characterization with the assistance of F.M. L.P. performed the FT-IR characterization and designed Figure 3, while J.T made macro-photography of the nuclei and designed Figure 1. F.M. wrote the manuscript with inputs from N.C., M.D.S and L.P. Figures 2, 4 and 5 were designed by F.M. and N.C.

ORCID

Nelly Schmitt http://orcid.org/0000-0002-6404-2643
Frédéric Marin http://orcid.org/0000-0001-8319-1735

REFERENCES

Awaji, M., & Suzuki, T. (1995). The pattern of cell proliferation during pearl sac formation in the pearl oyster. *Fisheries Science*, *61*, 747–751.

Cartier, L. E., & Krzemnicki, M. S. (2013). New developments in cultured pearl production: Use of organic and baroque shell nuclei. *Australian Gemmologist*, *25*, 6–13.

Caseiro, J. (1995) Evolution de l'épaisseur des dépôts de matériaux organiques et aragonitiques durant la croissance des perles de *Pinctada margaritifera*. Comptes-Rendus de l'Académie des Sciences de Paris *321* (ser. II), 9–16.

Clark, M. F., & Adams, A. N. (1977). Characteristics of the microplate method of enzyme-linked immunosorbent assay for the detection of plant viruses. *Journal of General Virology*, *34*, 475–483.

Cochennec-Laureau, N., Haffner, P., Levy, P., Saulnier, D., Langy, S., & Fougerouse, A. (2004). Development of antiseptic procedure to improve cultured pearl formation in *Pinctada margaritifera*. *Journal of Shellfish Research*, *23*, 285.

Cochennec-Laureau, N., Montagnani, C., Saulnier, D., Fougerouse, A., Levy, P., & Lo, C. (2010). A histological examination of grafting success in pearl oyster *Pinctada margaritifera* in French Polynesia. *Aquatic Living Resources*, *23*, 131–140.

De Paula, S. M., & Silveira, M. (2009). Studies on molluscan shells: Contributions from microscopic and analytical methods. *Micron*, *40*, 669–690.

Ellis, S., & Haws, M. (1999). *Producing pearls using the black-lip pearl oyster (Pinctada margaritifera)*. Center for Tropical and Sutropical Aquaculture Publication Number 141, 8p.

Erben, H. K. (1972). On the formation and growth of nacre. *Biomineralization Research Report*, *4*, 15–46.

Herbaut, C., Hui, B., Herbaut, J., Remoissenet, G., & Boucaud, E. (2000). La perle: l'isolement d'un corps étranger chez les mollusques nacriers. Evolution du greffon et du sac perlier, chez *Pinctada margaritifera* (mollusque, lamellibranche). *Bulletin de la Société Zoologique de France*, *125*, 63–73.

Hine, P. M., & Thorne, T. (2000). A survey of some parasites and diseases of several species of bivalve mollusc in northern Western Australia. *Diseases of Aquatic Organisms*, *40*, 67–78.

Humphrey, J. D. (2008). Disease and predation. In P. C. Southgate, & J. S. Lucas (Eds.), *The pearl oyster* (pp. 367–435). Oxford, UK: Elsevier.

Kanold, J. M., Guichard, N., Immel, F., Plasseraud, L., Corneillat, M., Alcaraz, G., … Marin, F. (2015). Spine and test skeletal matrices of the Mediterranean sea urchin *Arbacia lixula* – A comparative characterization of their sugar signature. *FEBS Journal*, *282*, 1891–1905.

Liu, C., Li, S., Kong, J., Liu, Y., Wang, T., Xie, L., & Zhang, R. (2015). In-depth proteomic analysis of shell matrix proteins of *Pinctada fucata*. *Scientific Reports*, *5*, 17269.

Mao Che, L., Le Campion-Alsumard, T., Boury-Esnault, N., Payri, C., Golubic, S., & Bézac, C. (1996). Biodegradation of shells of the black pearl oyster, *Pinctada margaritifera* var. *cumingii*, by microborers and sponges of French Polynesia. *Marine Biology*, *126*, 509–519.

Marie, B., Joubert, C., Tayalé, A., Zanella-Cléon, I., Belliard, C., Piquemal, D., … Montagnani, C. (2012). Different secretory repertoires control the biomineralization processes of prisms and nacre deposition of the pearl oyster shell. *Proceedings of the National Academy of Sciences of the United States of America*, *109*, 20986–20991.

Marie, B., Luquet, G., Pais De Barros, J. P., Guichard, N., Morel, S., Alcaraz, G., … Marin, F. (2007). The shell matrix of the freshwater mussel *Unio pictorum* (Paleoheterodonta, Unionoida). Involvement of acidic polysaccharides from glycoproteins in nacre mineralization. *FEBS Journal*, *274*, 2933–2945.

Marin, F. (2003). Molluscan shell matrix characterization by preparative SDS-PAGE. *The Scientific World Journal*, *3*, 342–347.

Marin, F., Amons, R., Guichard, N., Stigter, M., Hecker, A., Luquet, G., … Westbroek, P. (2005). Caspartin and calprismin, two proteins of the shell calcitic prisms of the Mediterranean fan mussel *Pinna nobilis*. *Journal of Biological Chemistry*, *280*, 33895–33908.

Marin, F., Gillibert, M., Wesbroek, P., Muyzer, G., & Dauphin, Y. (1999). Evolution: Disjunct degeneration of immunological determinants. *Geologie en Mijnbouw*, *78*, 135–139.

Marin, F., Le Roy, N., & Marie, B. (2012). The formation and mineralization of mollusc shell. *Frontiers in Biosciences*, *4*, 1099–1125.

Marin, F., Marie, B., Ben Hamada, S., Silva, P., Le Roy, N., Guichard, N., … Gueguen, Y. (2013). 'Shellome': Proteins involved in mollusk shell biomineralization – diversity, functions. In S. Watabe, K. Maeyama, & H. Nagasawa (Eds.), *Recent advances in pearl research* (pp. 149–166). Tokyo, Japan: Terrapub.

Marin, F., Muyzer, G., & Dauphin, Y. (1994). Caractérisation électrophorétique et immunologique des matrices organiques solubles de deux Bivalves Ptériomorphes actuels, *Pinna nobilis* L. et *Pinctada margaritifera* (L.). *Comptes-Rendus de l'Académie des Sciences de Paris*, *318* (Sér. II), 1653–1659.

Morrissey, J. H. (1981). Silver stain for proteins in polyacrylamide gels: A modified procedure with enhanced uniform sensitivity. *Analytical Biochemistry*, *117*, 307–310.

Nagai, K. (2013). The iridescence of pearls and the cultured-pearl industry. In S. Watabe, K. Maeyama, & H. Nagasawa (Eds.), *Recent advances in pearl research* (pp. 19–35). Tokyo, Japan: Terrapub.

Norton, J. H., Lucas, J. S., Turner, I., Mayer, R. J., & Newnham, R. (2000). Approaches to improve cultured pearl formation in *Pinctada margaritifera* through the use of relaxation, antiseptic application and incision closure during bead insertion. *Aquaculture*, *144*, 39–52.

Pavat, C., Zanella-Cléon, I., Becchi, M., Medakovic, D., Luquet, G., Guichard, N., … Marin, F. (2012). The shell matrix of the pulmonate land snail *Helix aspersa maxima*. *Comparative Biochemistry and Physiology Part B*, *161*, 303–314.

Petit, H., Davis, W., & Jones, R. (1980). A scanning electron microscopic study of the inorganic and organic matrices comprising the mature shell of *Amblema*, a fresh-water mollusc. *Tissue and Cell*, *12*, 581–593.

Rhee, S. H., & Tanaka, J. (2001). Synthesis of a hydroxyapatite/collagen/chondroitin sulphate nanocomposite by a novel precipitation method. *Journal of the American Ceramic Society*, *84*, 459–461.

Roberts, R. B., & Rose, R. A. (1989). Evaluation of some shells for use as nuclei for round pearl culture. *Journal of Shellfish Research*, *8*, 387–389.

Southgate, P. C. (2007). Overview of the cultured marine pearl industry. In: M. G. Bondad-Reantaso, S. E. McGladdery & F. C. J. Berthe (Eds.), *Pearl oyster health management: A manual* (pp. 7–17). Rome, FAO: FAO Fisheries Technical Paper N 503. 120p.

Strayer, D. L. (2008). *Freshwater mussel ecology - A multifactor approach to distribution and abundance*. Freshwater Ecology Series vol. 1, Berkeley, CA, USA: University of California Press.

Superchi, M., Castaman, E., Donini, A., Gambini, E., & Marzola, A. (2008). Nucleated cultured pearls: What is there inside? *Zeitschrift der Deutschen Gemmologischen Gesellschaft*, *57*, 33–40.

Taylor, J., & Strack, E. (2008). Pearl production. In P. C. Southgate, & J. S. Lucas (Eds.), *The pearl oyster* (pp. 273–302). Oxford, UK: Elsevier.

Tisdell, C., & Poirine, B. (2008). Economics of pearl farming. In P. C. Southgate, & J. S. Lucas (Eds.), *The Pearl Oyster* (pp. 473–495). Oxford, UK: Elsevier.

Weiss, I. M., Göhring, W., Fritz, M., & Mann, K. (2001). Perlustrin, a *Haliotis laevigata* (abalone) nacre protein, is homologous to the insulin-like growth factor binding protein N-terminal module of vertebrates. *Biochemical and Biophysical Research Commununications*, *285*, 244–249.

Westbroek, P., & Marin, F. (1998). A marriage of bone and nacre. *Nature*, *392*, 861–862.

Williams, S. T., Ito, S., Wakamatsu, K., Goral, T., Edwards, N. P., Wogelius, R. A., … Marsden, J. T. (2016). Identification of shell colour pigments in marine snails *Clanculus pharaonius* and *C. margaritarius* (Trochoidea; Gastropoda). *PLoS ONE*, *11*(7), e0156664.

How to cite this article: Schmitt N, Marin F, Thomas J, Plasseraud L, Demoy-Schneider M. Pearl grafting: Tracking the biological origin of nuclei by straightforward immunological methods. *Aquac Res*. 2018;49:692–700. https://doi.org/10.1111/are.13499